JOURNAL OF AGRICULTURAL AND FOOD CHEMISTRY

Kinetic Method for Determining Antioxidant Distributions in Model Food Emulsions: Distribution Constants of *t*-Butylhydroquinone in Mixtures of Octane, Water, and a Nonionic Emulsifier

LAURENCE S. ROMSTED* AND JIANBING ZHANG

Center for Advanced Food Technology and Department of Chemistry and Chemical Biology, Wright and Rieman Laboratories, Rutgers, The State University of New Jersey, New Brunswick, New Jersey 08903

The absence of reliable estimates of distributions of antioxidants in food emulsions hinders the development of a useful method for comparing the efficiencies of antioxidants. Here we describe the application of a pseudophase kinetic model, originally developed for homogeneous microemulsions, to the determination of distribution constants of *tert*-butylhydroquinone, TBHQ, in a fluid, opaque, model food emulsion composed of the nonionic emulsifier $C_{12}E_6$, octane, and water. This kinetic method should be applicable to a wide variety of charged and uncharged antioxidants in emulsions composed of charged and uncharged emulsifiers. The distribution constants for partitioning of TBHQ between the oil and surfactant film regions, K_O^I, and the aqueous and surfactant film regions, K_W^I, were obtained by fitting changes in first-order rate constants, k_{obs}, with emulsifier volume fraction for the reaction of 4-hexadecyl-2,6-dimethylbenzenediazonium ion, 16-ArN_2^+, with TBHQ. The rate of formation of the reduced arene product hexadecyl-2,6-dimethylbenzene, 16-ArH, was followed by HPLC. About 90% of the TBHQ is in the surfactant film at about 2% volume fraction of $C_{12}E_6$, which suggests that this region may be the primary site of antioxidant activity for neutral phenolic antioxidants.

KEYWORDS: Antioxidants; *tert*-butylhydroquinone; TBHQ; emulsion; nonionic emulsifier; nonionic surfactant; $C_{12}E_6$; HPLC; pseudophase kinetic model; kinetics; distribution constants

INTRODUCTION

Antioxidants have important functions in both emulsified foods (*1*−*5*) and biological systems (*1*, *6*, *7*). In foods, antioxidants slow the oxidation of unsaturated fats and oils and the concomitant formation of bad smells and tastes. In biological systems, antioxidants prevent the oxidation of a variety of compounds including lipids, proteins, DNA, and carbohydrates (*1*, *6*) and are important in minimizing the peroxidation of low-density lipoproteins (*7*). Antioxidants are believed to slow lipid oxidation in foods by breaking radical chain reactions that include the lipid, molecular oxygen, and peroxide intermediates (*3*, *4*, *5*).

One goal in food chemistry is to develop a scale of antioxidant activity for use in emulsified foods (*4*, *8*, *9*). However, establishing a scientific basis for selecting the best antioxidant for a particular application has proved refractory for a variety of reasons. Frankel and Meyer thoroughly examined the complexity of the problem in a recent review (*4*). They pointed out that selecting the most effective antioxidant for a particular food application requires understanding the true protective properties of the antioxidant, what substrates are being oxidized, where the antioxidant is located within the food, what is the effect of other components on the antioxidant activity, and the necessity for determining the relevance of a model system to a real food. They discussed the strengths and weaknesses of current antioxidant assays and their dependence on the selection of substrate, emulsifier type, and initiator. In sum, the complexity of the problem has to date prevented the development of an activity order for antioxidants that is independent of the assay used and the system studied.

One major factor that slows the development of a useful scale of antioxidant activity is inherent complexity of the multistepped free radical chain reactions of unsaturated lipids with molecular oxygen. The problem is exacerbated in organized systems, such as homogeneous aqueous micelles and microemulsions and biphasic emulsions, because the overall effectiveness of antioxidants also depends on the concentrations of the reactive components in the different regions in the system, that is, the aqueous and oil regions and the interfacial region composed of the surfactant film layered at the boundary between the aqueous and oil regions (*3*, *4*, *5*). Much progress has been made, but additional complexities still exist including fully understanding prooxidant (*10*−*13*) and synergistic activity (*14*, *15*).

* To whom correspondence should be addressed: 732-445-3639 (telephone); 732-445-5312 (fax); romsted@rutchem.rutgers.edu (e-mail).

10.1021/jf011711z CCC: $22.00
Published on Web 04/20/2002

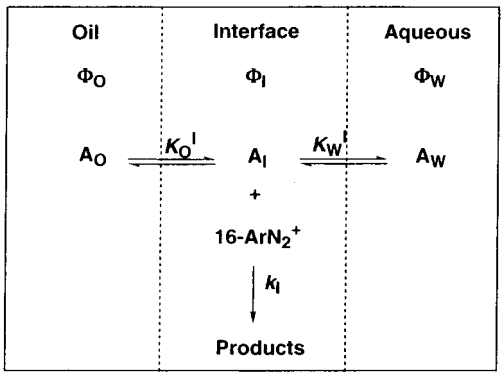

Figure 1. Representation of the oil, interface (or surfactant film), and aqueous regions of a microemulsion or an emulsion as indicated by the subscripts O, I, and W, respectively; Φ indicates the volume fraction of a region, A is the antioxidant, *K* is a distribution constant, k_I, is the rate constant for reaction of the arenediazonium ion, 16-ArN_2^+, with antioxidant in the interfacial region.

One approach to solving part of this problem is to determine the distribution of antioxidants within food emulsions (*3*−*5*). Unfortunately, modern spectrophotometric methods, such as NMR, ESR, fluorescence, or UV/Visible, that are often used to characterize micelles and microemulsions and to determine the distributions of small concentrations of components in homogeneous surfactant solutions (*16*, *17*), cannot be used in opaque emulsions. Antioxidant distributions in emulsions are often estimated by isolating and separately analyzing the compositions of the phases, for example, by centrifugation and ultrafiltration and using HPLC as the analytical technique (*18*−*21*). Recently, Stockmann and Schwarz combined ultrafiltration and dialysis techniques with a mathematical model to estimate the partitioning of low-molecular-weight compounds between the oil phase, aqueous phase, and the interfacial boundary between the two phases (*22*).

We decided to take a different approach by developing a method for estimating antioxidant distributions in model food emulsions based on well-established pseudophase kinetic models for chemical reactivity in homogeneous solutions of association colloids such as micelles, microemulsions, and vesicles (*17*, *23*−*25*). In pseudophase models, the totality of the oil, aqueous, and interfacial regions are assumed to act as separate reaction regions. The overall or observed rate is the sum of the rates in each region, and the distributions of reactive components (e.g., the antioxidant) between the regions are described by distribution constants. Fitting changes in the observed rate constant as a function of surfactant concentration with the equation for the model provides numerical values for the distribution constants and the rate constant for reaction in the surfactant film.

Here we apply the logic of pseudophase models to a system composed of two real phases and estimate the two distribution constants for partition of the antioxidant *tert*-butylhydroquinone, TBHQ, between the oil and interfacial, and water and interfacial, regions of a stirred, opaque, fluid, nonionic, emulsion composed of octane, water, and the emulsifier (hereafter called surfactant because it is highly purified) hexaethylene glycol mono dodecyl ether, $C_{12}E_6$ (**Figure 1**). We applied the pseudophase model to the measured observed first order rate constant, k_{obs}, as a function of $C_{12}E_6$ concentration for the reaction of the arenediazonium ion 4-hexadecyl-2,6-dimethylbenzenediazonium ion, 16-ArN_2^+, and TBHQ, **Scheme 1**, to estimate the distribution constants of TBHQ. Arenediazonium ions have a rich chemistry (*26*), but it can be controlled by proper selection of reactants and experimental conditions. The octane/$C_{12}E_6$/H_2O emulsion was chosen because we have substantial experience with it (*27*), because it is fluid, and because highly purified components are used to minimize potential problems caused by adventitious side reactions. We have used 16-ArN_2^+ extensively as a probe of the compositions of association colloid interfaces (*24*, *25*). Preliminary experiments demonstrated that 16-ArN_2^+ reacts with a variety of other antioxidants, including BHA, propyl gallate, ascorbic acid, and α-tocopherol (unpublished results), and that the distribution constant of TBHQ determined by spectral shift, kinetics, and the same sampling technique used in emulsions is the same within experimental error (*28*). TBHQ was selected as the model antioxidant because the mechanism of reaction of arenediazonium ions with 1,4-hydroquinone has been studied (*29*−*32*) and because we suspected that it would have measurable concentrations in all three regions of the emulsions based on known distribution constants of substituted benzenes and other small organic compounds (*17*).

The results reported here show that the kinetic method provides reasonable estimates of the two distribution constants of TBHQ in a nonionic emulsion of $C_{12}E_6$. The values obtained are in sensible agreement with those obtained in homogeneous $C_{12}E_6$ solutions of aqueous micelles and reverse microemulsions. The logic of the pseudophase model and the experimental approach is applicable to a wide variety of charged and uncharged antioxidants in emulsions composed of virtually any oil and neutral, anionic, and cationic surfactants over a wide range of solution pHs.

MATERIALS AND METHODS

Materials. HPLC-grade methanol, acetonitrile, and 2-propanol, *tert*-butylhydroquinone, TBHQ, (97%), succinic acid (99+%), 5,5-dimethyl-1-pyrroline *N*-oxide (DMPO (97%)), octane (99%), 2,6-di-*tert*-butyl-4-methylphenol (99%), *n*-butanol BuOH (99.8%), and inorganic reagents were purchased from Aldrich Chemical (Milwaukee, WI). Hexaethylene glycol mono dodecyl ether ($C_{12}E_6$ (98%)), was purchased from Fluka. All reagents were used as received except TBHQ, which was recrystallized three times from methanol. 4-*n*-Hexadecyl-2,6-dimethylbenzenediazonium tetrafluoroborate (16-ArN_2BF_4), 4-*n*-hexadecyl-2,6-dimethylbenzene (16-ArH), 4-*n*-hexadecyl-2,6-dimethylphenol (16-ArOH), and 4-n-hexadecyl-2,6-dimethylchlorobenzene (16-ArCl), were prepared earlier in our lab (*33*). All aqueous solutions were prepared by using distilled water that was passed over activated carbon and deionizing resin, and then redistilled.

General Methods. Product yields were measured by using computer-controlled Perkin-Elmer HPLCs equipped with diode array detectors and autosamplers fitted with Ranin C-18 reversed-phase columns (5-mm particle size, 4.6 mm i.d. × 25 cm) and 200-μL sample loops, and PE Nelson Turbochrom Version 4.1 software. UV spectra were obtained on either a thermostated Perkin-Elmer UV−Vis 559A or a Perkin-Elmer Lambda 40 UV−Vis spectrophotometer. Data accumulation and analyses were done on attached PC computers using Perkin-Elmer software. Solution pH was measured with an Orion combination pH microelectrode model 8103 with a Corning model 100 pH meter. All solutions were prepared with calibrated volumetric flasks, pipets, and syringes.

Determining k_{obs} for the Reaction of 16-ArN_2^+ and TBHQ in Octane/$C_{12}E_6$/Water Emulsions. Emulsions with volume ratios of aqueous solution to oil of 1:1 (10 mL aqueous solution to 10 mL octane) or 4:1 (16 mL aqueous solution to 4 mL octane) were equilibrated in a thermostated vessel. A single aqueous stock solution of 0.003 M HCl (pH 2.6) prepared by dilution of concentrated HCl was used in all reactions. The octane contained the $C_{12}E_6$, which ranged from 0.01 to 0.04 volume percent of the total emulsion volume of 20 mL. Vigorous stirring was maintained throughout the reaction period. The reaction vessel stood for about 15 to 20 min to ensure temperature equilibration at 25 °C. Reaction was initiated by adding sequentially, with syringes, freshly prepared aliquots of ice-cold stock solutions of 0.20 M TBHQ,

Scheme 1

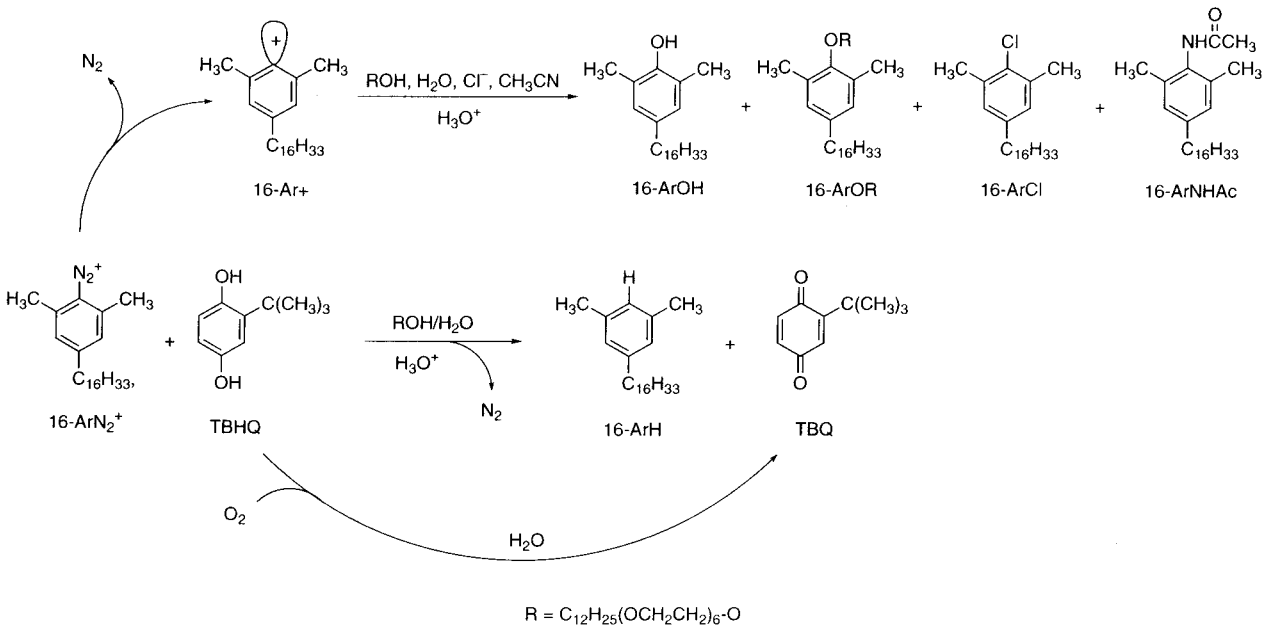

1.3 M DMPO, and 0.025 M 16-ArN_2BF_4 in CH_3CN giving, respectively, final concentrations (in moles per liter, M, of total emulsion volume) of 0.9 mM, 6.0 mM, and 1.2 mM. (Note: in the absence of antioxidants, 16-ArN_2^+ reacts with CH_3CN in the presence of water by a heterolytic mechanism to give an acetamide in small yields (*34*)). Reaction progress was monitored by periodically withdrawing 0.5-mL aliquots of the reaction mixture at selected time intervals and mixing them with 0.5 mL of 2.0 M HCl to quench the reaction between TBHQ and 16-ArN_2^+. These solutions stood in room temperature until sufficient octane vaporized to give transparent solutions. During this time period, about 72 h, the remaining 16-ArN_2^+ decomposed. Each sample was analyzed by HPLC to obtain the peak area, PA, of the reduced product, 16-ArH. The mobile phase for HPLC product separation was 2-propanol/methanol (25%:75%) with a flow rate of 1.0 mL per min, and the retention time for 16-ArH is 12−13 min. Absorbances were measured at 220 nm, and reported peak areas are averages of triplicate injections with an average deviation of about ± 1. Values of the observed rate constants, k_{obs}, of reaction between 16-ArN_2BF_4 and TBHQ were calculated from the slopes of $\ln(PA_{end}/(PA_{end} - PA))$ versus time plots, where PA is the peak area at any time *t*, and PA_{end} is the peak area at the end of the reaction. *R* is the correlation coefficient, generally = 0.98 (Supporting Information). We note that despite the uncertainty in concentration caused by air evaporation of the samples, the HPLC PA versus time profiles were smooth curves and those reactions that are cleanly first order give good correlation coefficients in their ln PA versus time plots showing that differential evaporation rates are not a serious problem. The distribution constants were obtained by iterative fitting (Origin 5.0) of k_{obs} versus volume fraction of $C_{12}E_6$ plots at the 1:1 and 4:1 water-to-oil phase volume ratios.

Determining K_O in Reverse Microemulsions by the Spectral Shift Method. A stock solution containing 87.1% octane, 11.52% $C_{12}E_6$, and 1.37% water by weight was added to a 10-mL volumetric flask. Sufficient BuOH was added by syringe to keep the final total molar ratio of BuOH to $C_{12}E_6$ at 19.3, and then octane was added to the 10-mL mark giving final $C_{12}E_6$ concentrations that ranged from 0.001 to 0.02 M. Exactly 3.0 mL of each solution was added to a cuvette, thermostated at 50 °C for about 5 min to thermally equilibrate the sample, and an aliquot of a freshly prepared stock solution of 0.092 M TBHQ in BuOH was added, giving a final TBHQ concentration of 3.0×10^{-4} M. The absorption spectrum of the sample was obtained between 200 and 400 nm. The absorbance, *A*, at 308 nm was recorded, and the cmc was estimated from the break in the A−$C_{12}E_6$ profile. The binding constant, K_O, was obtained from the slope of a plot $(A - A_o)/(C_{12}E_6 -$ cmc) versus *A* where A_o is the absorbance in the absence of TBHQ. This equation is based on a standard method for estimating binding constants from shifts in absorbance spectra (*35*).

LOGIC OF THE KINETIC METHOD

The mathematical treatment for the rate of reaction of 16-ArN_2^+ with TBHQ in emulsions is based on treatments developed for reactions in micelles (*36*−*38*) and in microemulsions (*39*, *40*). The crucial elements of the treatment are summarized below and in **Figure 1**. The derivation of the rate expression (see below) is in the Supporting Information, Appendix I.

In pseudophase models for homogeneous microemulsions (*39*, *40*), in which the internal structure may be oil-in-water droplets, bicontinuous, or water-in-oil droplets, the totality of the solution is divided into oil, surfactant film, and water regions with the surfactant lining the boundary between the oil and water regions, **Figure 1**. Each region is treated as a separate phase or pseudophase, and the partitioning of components between the regions depends on their free energies of transfer between the pseudophases. The rate of transfer of reactants is assumed to be much faster than the observed rate of the reaction, such that the distribution of the reactants is always at dynamic equilibrium throughout the time course of the reaction. Here this model is applied to stirred biphasic emulsions, in which the distributions of TBHQ and 16-ArN_2^+ between the three regions are also assumed to be in dynamic equilibrium, and the observed rate of reaction is the sum of the rates in the oil, interfacial, and aqueous regions. The low concentrations of reactants are assumed to minimally perturb the properties of the emulsion interface, as is commonly assumed in pseudophase kinetic models. Because the substrate, 16-ArN_2BF_4, is itself a water insoluble surfactant, we assume that its hydrocarbon tail and cationic headgroup orient it at the oil−water boundary along with the nonionic surfactant $C_{12}E_6$, and that its concentration in the aqueous and oil regions is negligible (*25*). The reactions are carried out under first-order conditions, i.e., the stoichiometric concentration of the second reactant, TBHQ, is in large excess over that of 16-ArN_2^+ such that the concentration of TBHQ does not change significantly throughout the time course of the reaction. Under these conditions, the observed second-

Table 1. Normalized Yields of Reaction of 16-ArN_2^+ and TBHQ in $C_{12}E_6$ Aqueous Micelles at 30 °C

		10^3•reactant concentrations (M)				normalized yields (%)		
buffer	pH	[DMPO]	[TBHQ]	[$C_{12}E_6$]	[16-ArN_2^+]	16-ArH	16-ArOH	16-ArCl
0.003 M HCl	2.58	7.75	0.887	2.69	0.117	100	0	0
0.003 M HCl	2.58	7.75	0.887	13.4	0.117	100	0	0
1.0 M HCl[a]		8.62	0.904	10.25	0.0650	3.57	76.3	20.1
2.0 M HCl[a]		8.62	0.904	10.25	0.0650	1.33	66.4	32.3

[a] 16-ArOR also forms in $C_{12}E_6$ micelles under these conditions in small but reproducible yield and does not have a significant effect on the product distribution in competitive heterolytic dediazoniation reactions (*34*). In 1.0 and 2.0 M HCl the average yields of 16-ArOR obtained from triplicate injections are 1.29% and 1.20%, respectively.

order rate constant depends only on the rate constant for reaction in the interfacial region, k_I, and on the concentration of TBHQ in the interfacial region (or surfactant film), ($TBHQ_{sf}$), in mol/L of interfacial volume, but NOT on the stoichiometric concentration of antioxidant in total emulsion volume, [$TBHQ_{sf}$], or in the aqueous phase. The rate of reaction of TBHQ with 16-ArN_2^+, or of any other pair of molecules in the interfacial region of micelles, microemulsions, or emulsions, depends on its concentration in that region, and that concentration may be significantly greater, e.g., 1−2 orders of magnitude, than its stoichiometric concentration (*17*, *24*, *25*, *38*).

The concentration of TBHQ in the interfacial region is described by two partition constants: one between the oil and interfacial regions, P_O^I, and one between the aqueous and interfacial regions, P_W^I, **Figure 1**. Partition constants are used in the derivation because the oil, water, and surfactant components are measured by volume, and because the total volume of surfactant is a small fraction of the total emulsion volume. Partition constants are converted distribution constants, K_O^I and K_W^I, for comparison with distribution constants determined in homogeneous micelles and microemulsions. The dependence of k_{obs} and the second-order rate constant, k_2, on the phase volumes of oil, surfactant, and water are given by the following (see also Supporting Information):

$$k_{obs} = k_2[TBHQ_T] = \frac{[TBHQ_T]k_I K_O^I K_W^I}{\Phi_O K_W^I V_m + \Phi_I K_O^I K_W^I + \Phi_W K_O^I V_m} \qquad (1)$$

where [$TBHQ_T$] is the stoichiometric concentration of TBHQ in the emulsion and it is related to the TBHQ concentrations in the aqueous, oil, and surfactant film regions by a mass balance equation.

Eq 1 predicts that k_{obs}, and k_2 at constant [$TBHQ_T$], decrease with the increasing volume fraction (%) of the surfactant, Φ_I, when the phase volume ratio of oil (Φ_O) to water (Φ_W) is held constant. Both distribution constants, K_O^I and K_W^I, are unknown, and to estimate their values at least two data sets of k_{obs} (or k_2) versus Φ_I at two different Φ_W/Φ_O ratios must be solved as two equations in two unknowns (see below). The value for V_m, the molar volume of the reaction region, must also be selected (see below).

RESULTS

Scheme 1 shows the competing reactions of 16-ArN_2^+ in dilute aqueous acid in the absence of light, and in the presence and absence of TBHQ. The evidence for the chemistry in **Scheme 1** is discussed below. In the presence of TBHQ the dominant reaction is reduction of 16-ArN_2^+ to 16-ArH and oxidation of TBHQ to TBQ. In the absence of autocatalysis (see below), this reaction is second-order overall, first order in 16-ArN_2^+ and in TBHQ; the overall stoichiometry is 2 equiv arenediazonium ion reduced per equiv TBHQ oxidized, and the proposed mechanism (*29*, *31*) is a series of single electron transfer reactions (see Discussion). This reaction is significantly faster than the heterolytic dediazoniation reaction (*26*) that gives products from reaction with weakly basic nucleophiles and also the reaction of TBHQ with dissolved O_2. The nucleophiles in octane/$C_{12}E_6$/water emulsions and the quenching solution are the following: CH_3CN in the 16-ArN_2^+ stock solution, H_2O, the terminal OH group of $C_{12}E_6$, and Cl^- in the HCl in the quenching solution. All products from these reactions have been identified previously (*25*).

The experimental protocol for measuring k_{obs} for the reaction of 16-ArN_2^+ with TBHQ is straightforward. Aliquots of the aqueous phase containing 0.003 M HCl and octane containing $C_{12}E_6$ are added to a covered, stirred, thermostated, vessel. An opaque, fluid mixture is formed. Ice-cold stock solutions of TBHQ, DMPO, and 16-ArN_2BF_4 in CH_3CN are added sequentially. Addition of 16-ArN_2BF_4 initiates the reaction. Reaction progress is monitored by periodically withdrawing 0.5-mL aliquots of the reaction mixture at selected time intervals, and immediately mixing each aliquot with a 0.5-mL solution of 2 M HCl in an HPLC vial. Typically, 25 samples are taken from each reaction mixture. The 1 M HCl in this mixture quenches the reaction of 16-ArN_2^+ with TBHQ, and the remaining 16-ArN_2^+ decomposes via the heterolytic mechanism. The 25 quenched reaction mixtures sit for about 72 h in open vials. During this time sufficient octane evaporates to give homogeneous solutions, and the concentration of 16-ArH in each is analyzed by HPLC. Reported concentrations of reagents in the emulsions are expressed in mol per L (molar) of total emulsion volume (i.e., the sum of the water and aqueous phases in the reaction mixture prior to evaporation). The reactions were monitored for at least 2 half-lives, and the correlation coefficients, R, for the ln PA (peak area) versus times plots were all $\geq$ 0.98.

The above protocol is based on a series of experiments that established the optimal pH, that minimized the competing (but much slower) reaction of TBHQ with O_2, and that showed that the reaction of 16-ArN_2^+ with TBHQ is quenched in strong acid. The competing reaction of TBHQ with O_2 is on the order of 100 times slower than the reaction of TBHQ with 16-ArN_2^+. Thus, the reaction with 16-ArN_2^+ and k_{obs} does not include a significant contribution from the reaction of TBHQ with O_2. Details on the reaction of TBHQ with O_2 are in Appendix II in the Supporting Information.

Two sets of experiments, **Table 1**, were run in aqueous $C_{12}E_6$ micelles at 30 °C that showed that the strong acid quenches the reaction between 16-ArN_2^+ and TBHQ. In 2.7 and 13.4 mM $C_{12}E_6$ micellar solutions containing 0.001 M HCl, the only peak in the HPLC chromatograms is for 16-ArH, and no peak is observed for 16-ArOH, which is the most probable other product. When the reaction was carried out at much higher acidity, i.e., 1 and 2 M HCl, the product yields are typical of those from heterolytic dediazoniations in the absence of reducing

Table 2. First Order Rate Constant, k_{obs}, for Reaction of 16-ArN_2^+ with TBHQ in $C_{12}E_6$ Emulsions Containing 1:1 and 4:1 Water to Octane Volume Ratios at 25 °C[a]

1:1 H_2O/octane vol/vol[b]		4:1 H_2O/octane vol/vol[c]	
$C_{12}E_6$ vol fraction (%)	10^3k_{obs} (s^{-1})	$C_{12}E_6$ vol fraction (%)	10^3k_{obs} (s^{-1})
0.986	3.01	1.03	2.91
1.49	2.42	1.27	1.89
2.01	1.67	1.52	1.58
2.47	1.42	1.73	1.40
3.00	1.14[d]	1.97	1.28
3.54	0.806[d]	2.23	1.30
4.12	0.851[d]	2.48	0.957
		2.95	0.839[d]
		3.42	0.699[d]
		3.92	0.716[d]

[a] Rate profiles for each k_{obs} value are in the Supporting Information. [b] Emulsions were composed of 10.0 mL of octane containing the indicated volume percent of $C_{12}E_6$, 10.0 mL of aqueous 0.003 M HCl, and 0.146 mM 16-ArN_2^+, 0.911 mM TBHQ, and 3.73 mM DMPO. All concentrations are based on the total volume of the emulsion. [c] Emulsions were composed of 4.0 mL of octane containing the indicated volume percent of $C_{12}E_6$, 16.0 mL of aqueous 0.003 M HCl, and 0.151 mM 16-ArN_2^+, 0.911 mM TBHQ, and 4.98 mM DMPO. All concentrations are based on the total volume of the emulsion. [d] Value of k_{obs} obtained from the initial slope (see text).

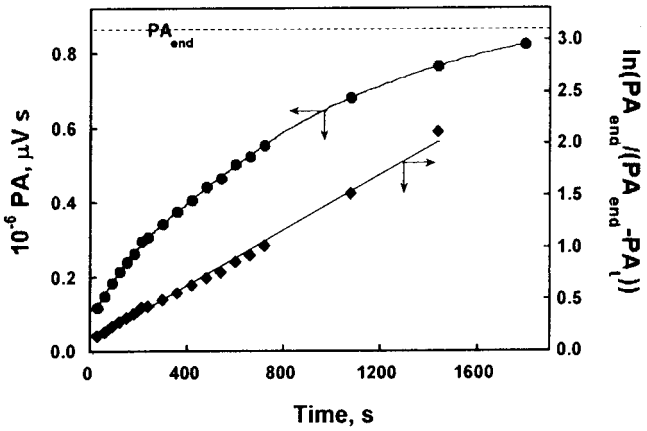

Figure 2. Peak area, PA, versus time and ln PA plots versus time for reaction of 16-ArN_2^+ with TBHQ at 25 °C in emulsions composed of 4:1 aqueous 0.003 M HCl to octane volume ratio at low (1.52%) $C_{12}E_6$. At the end of the reaction: $PA_{end} = 0.869$ (dotted line). The emulsions contained 0.151 mM 16-ArN_2^+, 0.911 mM TBHQ, and 4.98 mM DMPO. The correlation coefficient for the ln PA versus time plot is 0.994 and $k_{obs} = 0.00158\ s^{-1}$ ($R = 0.994$).

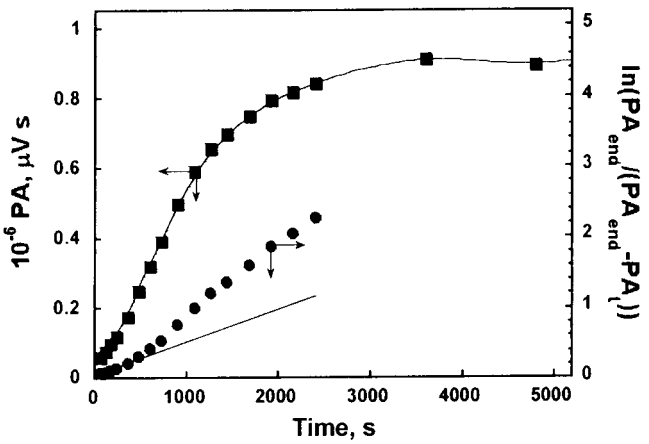

Figure 3. Peak area, PA, versus time and ln PA plots versus time for reaction of 16-ArN_2^+ with TBHQ at 25 °C in emulsions composed of 4:1 aqueous 0.003 M HCl to octane volume ratio at high (3.92%) $C_{12}E_6$. At the end of the reaction: $PA_{end} = 0.9$. The emulsions contained 0.151 mM 16-ArN_2^+, 0.911 mM TBHQ, and 4.98 mM DMPO. The correlation coefficient for the initial slope of the ln PA versus time plot is 1.000 and $k_{obs} = 0.000716\ s^{-1}$ ($R = 1.000$).

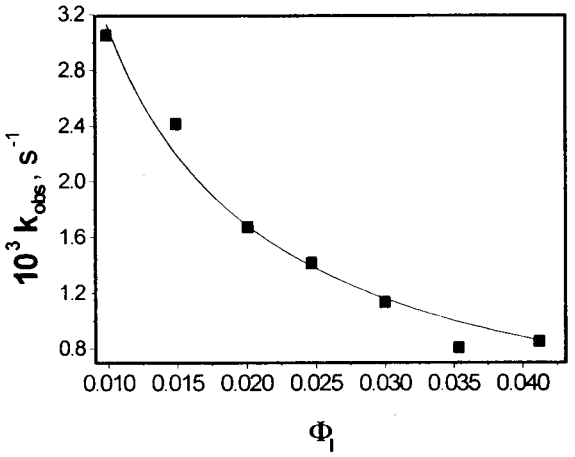

Figure 4. Plot of k_{obs} versus the volume fraction, Φ_I, of $C_{12}E_6$ (%) in emulsions of 1:1 volume ratio of aqueous 0.003 M HCl to octane at 25 °C. The emulsions contained 0.146 mM 16-ArN_2^+, 0.911 mM TBHQ, and 3.73 mM DMPO. The solid line was obtained by iterative fit of the data using eq 2 and the software package Origin. Parameters from the fitting are in **Table 3**.

agents (*25*, *34*). Note the high total yields of 16-ArOH and 16-ArCl. The small yields of 16-ArH come from the reduction of unreacted 16-ArN_2^+ by the 16-ArOH product (*34*). These results demonstrate that strong acid quenches the reaction of 16-ArN_2^+ with TBHQ, and that the 16-ArH yield can be measured as a function of time by periodic sampling of the reaction mixture as shown previously (*28*).

Table 2 lists the first-order rate constants for reaction of 16-ArN_2^+ with TBHQ in emulsions of 1:1 and 4:1 water/octane volume ratios at the indicated percentages of $C_{12}E_6$. As noted above, the rate constant for reaction of arenediazonium ions with hydroquinones is pH dependent, because it is the mono anion and not the neutral form of a hydroquinone that reacts with arenediazonium ions (*29*). Indeed, in the emulsions the pH had to be set at about 2.5 (0.003 M HCl) so that the reaction was slow enough to obtain a sufficient number of samples during the time course of the reaction. All the rate constants were obtained by the protocol described above. **Figure 2** shows a typical 16-ArH peak area, PA, versus time and a first-order ln PA versus time plot for a reaction that is first-order throughout the time course of the reaction. **Figure 3** shows a typical 16-ArH PA versus time and first-order ln PA versus time plot for reactions a higher $C_{12}E_6$ concentrations that were non first order, i.e., after an initial slow period the rate of the reaction accelerates. Similar biphasic plots were observed in solutions of aqueous $C_{12}E_6$ micelles at high $C_{12}E_6$ concentrations (not shown). Autocatalysis in emulsions under some conditions is consistent with the published mechanism of the reaction (*29*, *31*), which is also autocatalytic under some conditions (see Discussion) (*31*). A value of k_{obs} was obtained by drawing the best straight line through the initial set of data points as illustrated in **Figure 3**. This procedure gives sensible estimates of the association constants for TBHQ.

Figures 4 and **5** show plots of the decrease in k_{obs} with increasing $C_{12}E_6$ concentration from the data for 1:1 and 4:1 molar ratios of water to oil listed in **Table 2**. The curves were

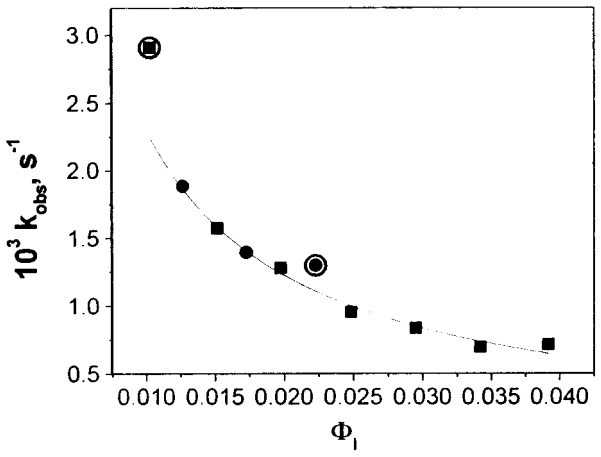

Figure 5. Plot of k_{obs} versus the volume fraction, Φ_I, of $C_{12}E_6$ (%) in emulsions of 4:1 volume ratio of aqueous 0.003 M HCl to octane at 25 °C. The emulsions contained 0.151 mM 16-ArN_2^+, 0.911 mM TBHQ, and 4.98 mM DMPO. The filled circles and squares represent two different runs. The solid line was obtained by iterative fit of the data using eq 2 and the software package Origin. The larger open circles are two data points that were not included in the simulation because they are too far from the basic curve. Parameters from the fitting are in **Table 3**.

Table 3. Fitting Parameters Obtained by Applying Equation 2 to the k_{obs} versus Φ_I Plots in **Figures 4** and **5**; and the Distribution Constants in Emulsions, K_W^I, and K_O^I, at 25 °C and Distribution Constants in Aqueous Micelles, K_W, at 30 °C and Reverse Micelles, K_O, at 50 °C; and the Percentage of TBHQ (%$TBHQ_{sf}$) in the Surfactant Film of the Emulsion under One Set of Conditions

	fitting parameters	
H_2O/octane, vol/vol	*a*	*b*
1/1	18.9	509
4/1	21.5	827
	distribution constants (M^{-1})	
interface/H_2O	$K_W^I = 637$	$K_W = 303$[a]
interface/octane	$K_O^I = 140$	$K_O = 198$[b]
%$TBHQ_{sf}$	91.2% at 2.01% $C_{12}E_6$[c]	

[a] Distribution constant in aqueous micelles. An average of 8 determinations at 30 °C from pH 2.58 to 4.65 by three different methods with an average deviation of 1.5% (*28*). [b] Distribution constant in reverse microemulsions at 50 °C, see text for details. [c] In 1:1 molar ratio of octane to water emulsion.

obtained by iterative fits with eq 2 using the program Origin

$$y = \frac{a}{1 + bx} \quad (2)$$

where $y = k_{obs}$ and $x = \Phi_I$. The fitting parameters *a* and *b* are mathematically related to the terms in eq 1 (see Supporting Information, Appendix I). The estimated values of *a* and *b* are listed in **Table 3**. The two values of *b* were used with the equation for *b* to obtain values for K_W^I and K_O^I by solving two equations in two unknowns. The molar volume of reaction, V_m, is not known explicitly (eq 1), and its value is usually assumed to be equal to the molar volume of the interfacial region (*41*) with nonionic surfactants, the layer created by the polyoxyethylene headgroups, or the molar volume of both the headgroups and tails (*42*); i.e., the reaction occurs anywhere within the volume of the surfactant film in the emulsions. For simplicity, we set $V_m = 0.45\ M^{-1}$ (the volume of 1 mol $C_{12}E_6$ in 1 L of solution, assuming that $C_{12}E_6$ has a density of 1 kg m^{-3} (*17*, *24*, *25*)), and we used this value to estimate the

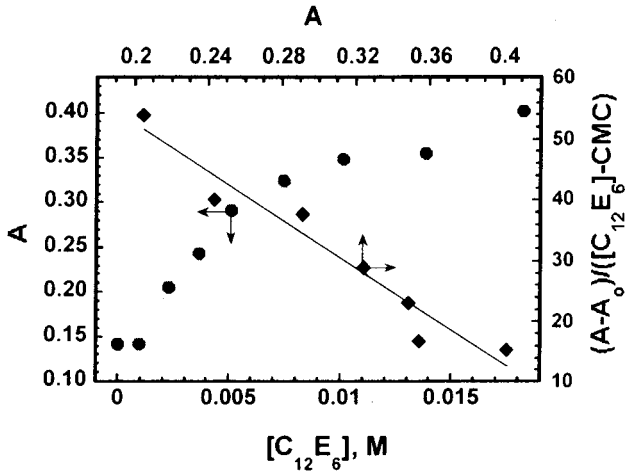

Figure 6. Effect of added $C_{12}E_6$ on the absorbance, A, of TBHQ in octane/$C_{12}E_6$/*n*-butanol/water microemulsions at 50 °C. The break in the profile at 0.0011 M is assumed to equal the cmc. The linear plot of the data fits the equation $y = 92.1 - 198x$; $R = 0.945$.

distribution constants listed in **Table 3**. If V_m were set equal to the smaller molar volume of the headgroup region, the values of the distribution constants would be proportionately smaller, but the basic conclusions would be unaffected. The values of K_W^I and K_O^I are also listed in **Table 3** along with the distribution constants for TBHQ in aqueous $C_{12}E_6$ micelles, K_W, and in reverse microemulsions, K_O, of octane/$C_{12}E_6$/BuOH/H_2O. In aqueous $C_{12}E_6$ micelles, $K_W = 303 \pm 1.5\%$ for 8 determinations by three separate methods, including HPLC which was carried out to demonstrate the viability of the sampling method by comparing it with more standard methods (*28*).

K_O in the reverse microemulsions was estimated by the spectral shift method and the results are shown in **Figure 6**. The absorbance, A, increases steadily with added $C_{12}E_6$ above the cmc and approaches a plateau. To minimize the partitioning of TBHQ into the aqueous water pools of the reverse microemulsion, the water-to-surfactant ratio was kept as low as possible ($H_2O/C_{12}E_6 = 2.96$). Plotting these data by a standard method (see Materials and Methods) (*35*) gives a straight line and the slope is K_O. To prevent phase separation, the experiment had to be carried out at 50 °C and with significant amounts of added BuOH.

DISCUSSION

The results in **Table 3** demonstrate that the pseudophase kinetic model for second order reactions in fluid, opaque emulsions provides reasonable estimates of the distribution constants of TBHQ between the oil and interfacial and aqueous and interfacial regions. The values of distribution constants are similar to those obtained in homogeneous solutions of aqueous micelles and reverse microemulsions. In both systems, the distribution constants for TBHQ between the oil and interfacial regions are smaller than those between the aqueous and interfacial regions. Exact agreement would be surprising and probably coincidental. The temperatures in the experiments are different, 25 °C in the emulsions and 30 and 50 °C in the aqueous micelles and reverse microemulsions, respectively, although equilibrium constants are not nearly as temperature sensitive as rate constants. In addition, BuOH had to be added to the reverse microemulsions to ensure that the solution was homogeneous. The hydration number of the polyoxyethylene chain region of emulsion droplets is significantly lower than that of aqueous micelles of $C_{12}E_6$ (*27*), and BuOH and nonionic

Scheme 2

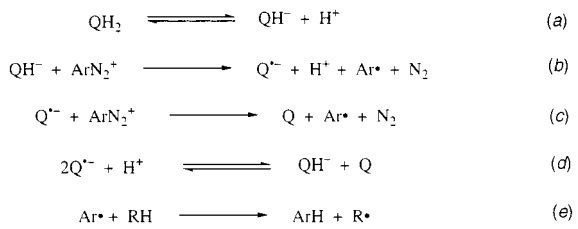

surfactants also partition into the oil phase (*43*, *44*) which may change the medium properties of the interfacial region. Thus, the polarity and the solubility properties of TBHQ in the interfacial regions of emulsions, micelles, and microemulsions are probably different and the distribution constants need not be the same.

Table 3 also illustrates that the percentage of $TBHQ_{sf}$ in the surfactant film of the emulsions is very high ($\%TBHQ_{sf} = 91.2$ (see Supporting Information, Appendix I for the calculation)) in the interfacial region of the emulsions of 2% $C_{12}E_6$ and a 1:1 water-to-octane ratio. The value of $\%TBHQ_{sf}$ depends on both the $C_{12}E_6$ concentration and the water-to-octane ratio. $\%TBHQ_{sf}$ varies from 83.5 to 95.6% at 1:1 water/octane and 89.2 to 97.1% in 4:1 water/octane from the lowest to highest $\%C_{12}E_6$ used at each ratio, **Table 2**. Similar equations give 7.2% TBHQ in the oil and 1.6% in both the aqueous region and oil region of 1:1 water/octane emulsions, and 2.7% and 3.1% TBHQ, respectively, in the aqueous and octane regions of 4:1 water/octane emulsions. The high fraction (ca. 90%) of TBHQ in the interfacial region suggests that the primary region of activity of phenolic antioxidants is in the interfacial region of food emulsions. Smaller, but still significant concentrations (on the order of 50%), of some phenolic compounds were estimated to be located in the interfacial region of SDS emulsions (*22*). Strongly hydrophobic antioxidants such as tocopherols may be primarily in the oil region, but charged antioxidants such as ascorbic acid (at neutral pH) are probably primarily in the aqueous phase, although their distribution will probably depend on both pH and surfactant charge. Distribution constants of these and many other antioxidants can be measured by the kinetic method.

Several factors affect the precision of the k_{obs} values and the ease of use of the kinetic method: (a) the competing reaction of TBHQ with dissolved O_2; (b) the apparent autocatalytic reaction at high $C_{12}E_6$ concentration; and (c) the substantial time required to measure a value for k_{obs} by HPLC. The proposed mechanism of reaction of 1,4-hydroquinone, catechol, and catechol derivatives (and presumably TBHQ) with dissolved O_2 is complex (*45*), and a number of high-energy intermediates (such as semiquinone radical anion and superoxide, $O_2^{\bullet -}$) form during the reaction. We assume that DMPO scavenges such intermediates, primarily in the aqueous phase, thus slowing the reaction of TBHQ with dissolved O_2 so that the TBHQ concentration remains constant throughout the time course of the reaction of 16-ArN_2^+ with TBHQ at low $C_{12}E_6$ concentrations.

At higher $C_{12}E_6$ concentrations, the reactions become autocatalytic **Figure 3**. Autocatalysis is consistent with the proposed multistepped mechanism for the reaction of arenediazonium ions with reducing agents such as 1,4-hydroquinone, catechol, and their derivatives (*29*, *31*), as shown in **Scheme 2**. Reactions *a* to *e* of this mechanism account for the pH dependence of the reaction, the overall second-order kinetics, and for the observed 2 ArN_2^+ to 1 QH_2 stoichiometry for the formation of Q and ArH. The reactive form of the QH_2 is its mono anion, QH^-, as shown by the decrease in the observed rate with increasing acidity (*29*). We observed similar decreases in rate with increasing acidity in micelles and emulsions. Reaction *b* is rate-determining because reactions *c* and *d* are assumed to be very fast (*46*). The 2:1 stoichiometry is observed because at the end of the reaction 2 molecules of ArN_2^+ are reduced to ArH for each molecule of QH_2 oxidized to Q (reactions *b*, *c*, and *e*). Product (ArH) is known to form in a fast step with CH_3CN (*30*). CH_3CN is added as the carrier solvent for 16-ArN_2BF_4 in these experiments and is ca. 1% of the total emulsion volume. Autocatalysis in these reactions is attributed to comproportionation (back reaction of disproportionation reaction *d*) of quinone and unreacted quinone mono anion to give two semiquinone radical anions (*31*). The increase in $Q^{\bullet -}$ concentration enhances the contribution of reaction *c*, speeds the formation of Q, and increases the rate of ArH formation until the reaction becomes autocatalytic. The appearance of autocatalysis at elevated $C_{12}E_6$ concentrations in micelles (*28*) and emulsions (**Table 2** and **Figure 3**) is consistent with this mechanism. In general, the rates of reactions in micelles and microemulsions depend on the concentrations of the reactants in the aqueous, oil, and interfacial regions and their rate constants within those regions (*37*). The concentrations of reactants in each region depend on their distribution constants between the regions. The same factors should operate in emulsions. At higher $C_{12}E_6$ concentrations, binding of QH^- and Q increases their concentrations sufficiently to make comproportionation significant and speed reactions *b*, *c*, and *e*.

The results in **Figures 4** and **5** and **Table 3** demonstrate the viability of the kinetic method for determining the distribution constants of antioxidants in opaque emulsions. The imprecision in the estimate of k_{obs} caused by autocatalysis can be minimized by restricting the measurements to surfactant concentrations below the appearance of autocatalysis and by obtaining more k_{obs} values. Another alternative is to monitor the reaction of 16-ArN_2^+ with an antioxidant electrochemically. Following phenolic antioxidant reactions electrochemically is now routine (*47*), including in reverse micelles (*48*) and TBHQ in emulsions (*49*), and loss of arenediazonium ion has been monitored electrochemically (*50*−*52*), including the reaction of 16-ArN_2^+ with TBHQ in octane/H_2O/$C_{12}E_6$ emulsions (unpublished results). Electrochemical methods also permit continuous monitoring of reactions that are substantially faster than those monitored by the sampling technique and rapid analysis of the data to obtain k_{obs}.

The next steps in this project are to demonstrate that distribution constants can be determined in more food-like emulsions using food emulsifiers and purified triglyceride oils (stripped of their natural antioxidants), to determine the effects of surfactant charge, and to apply the method to a variety of antioxidants to look for structure distribution constant correlations. Kinetic models are available for treating reactions in solutions of ionic surfactants such as sodium dodecyl sulfate and cetyltrimethylammonium bromide (*53*), and treatments are available for estimating the distribution constants of ionizable compounds as a function of pH (*54*−*56*) that are applicable to antioxidants such as ascorbic acid or Trolox C. Finally, each time a distribution constant for an antioxidant is estimated, the experiment also provides an estimate of the rate constant (k_I in **Scheme 1** and **Figure 1**) for reaction in the interfacial region of the emulsion. Comparison of these rate constants for a variety of antioxidants may eventually lead to a scale of antioxidant activity.

ACKNOWLEDGMENT

We thank Dr. Donald Hamm of Best Foods and Carlos Bravo-Diaz and Elisa Gonzalez-Romero for extremely fruitful discussions.

Supporting Information Available: Appendix I, derivation of eq 1; Appendix II, reaction of TBHQ and O_2, includes Tables AII-1 to AII-4 and Figures AII-1 to AII-4. Figures SI-1 to SI-17 are the kinetic data used to estimate the values of k_{obs} in **Table 2**. This material is available free of charge via the Internet at http://pubs.acs.org.

LITERATURE CITED

(1) Halliwell, B.; Aeschbach, R.; Loliger, J.; Aruoma, O. I. The Characterization of Antioxidants. *Food Chem. Toxicol.* **1995**, *33*, 601−617.

(2) Frankel, E. N. Antioxidants in Lipid Foods and Their Impact on Food Quality. *Food Chem.* **1996**, *57*, 51−55.

(3) Coupland, J. N.; McClements, D. J. Lipid Oxidation in Food Emulsions. *Trends Food Sci. Technol.* **1996**, *7*, 83−91.

(4) Frankel, E. N.; Meyer, A. S. The Problems of using One-dimensional Methods to Evaluate Multifunctional Food and Biological Antioxidants. *J. Sci. Food Agric.* **2000**, *80*, 1925−1941.

(5) McClements, D. J.; Decker, E. A. Lipid Oxidation in Oil-in-Water Emulsions: Impact of Molecular Environment on Chemical Reactions in Heterogeneous Food Systems. *J. Food Sci.* **2000**, *65*, 1270−1282.

(6) Halliwell, B. Free Radicals and Antioxidants: A Personal View. *Nutr. Rev.* **1994**, *52*, 253−274.

(7) Bowry, V. W.; Ingold, K. U. The Unexpected Role of Vitamin E (α-Tocopherol) in the Peroxidation of Human Low-Density Lipoprotein. *Acc. Chem. Res.* **1999**, *32*, 27−34.

(8) Pryor, W. A.; Cornicelli, J. A.; Devall, L. J.; Tait, B.; Trivedi, B. K.; Witiak, D. T.; Wu, M. A Rapid Screening Test to Determine the Antioxidant Potencies of Natural and Synthetic Antioxidants. *J. Org. Chem.* **1993**, *58*, 3521−3532.

(9) Ruberto, G.; Baratta, M. T. Antioxidant Activity of Selected Essential Oil Components in Two Lipid Model Systems. *Food Chem.* **2000**, *69*, 167−174.

(10) Aruoma, O. I. Assessment of Potential Prooxidant and Antioxidant Actions. *J. Am. Oil Chem. Soc.* **1996**, *73*, 1617−1625.

(11) Roedig-Penman, A.; Gordon, M. H. Antioxidant Properties of Catechins and Green Tea Extracts in Model Food Emulsions. *J. Agric. Food Chem.* **1997**, *45*, 4267−4270.

(12) Huang, S.-W.; Satue-Gracia, M. T.; Frankel, E. N.; German, J. B. Effect of Lactoferrin on Oxidative Stability of Corn Oil Emulsions or Liposomes. *J. Agric. Food Chem.* **1999**, *47*, 1356−1361.

(13) Mei, L.; McClements, D. J.; Decker, E. A. Lipid Oxidation in Emulsions as Affected by Charge Status of Antioxidants and Emulsion Droplets. *J. Agric. Food Chem.* **1999**, *47*, 2267−2273.

(14) Larsen, E.; Abendroth, J.; Partali, V.; Schulz, B.; Sliwka, H.-R.; Quartey, E. G. K. Combination of Vitamin E with a Carotenoid: α-Tocopherol and Trolox Linked to β-apo-8′-carotenoic Acid. *Chem. Eur. J.* **1998**, *4*, 113−117.

(15) Zhou, B.; Jia, Z.-S.; Chen, Z.-H.; Yang, L.; Wu, L.-M.; Liu, Z.-L. Synergistic Antioxidant Effect of Green Tea Polyphenols with α-Tocopherol on Free Radical Initiated Peroxidation of Linoleic Acid in Micelles. *J. Chem. Soc., Perkin Trans. 2* **2000**, 785−791.

(16) *Surfactant Solutions: New Methods of Investigation*; Zana, R., Ed.; Marcel Dekker: New York, 1985.

(17) Savelli, G.; Germani, R.; Brinchi, L. Reactivity Control by Aqueous Amphiphilic Self-Assembling Systems. In *Reactions and Synthesis in Surfactant Systems*; J. Texter, Ed.; Marcel Dekker: New York, 2001; pp 175−246.

(18) Huang, S.; Frankel, E. N.; Aeschbach, R.; Greman, J. B. Partition of Selected Antioxidants in Corn Oil−Water Model Systems. *J. Agric. Food Chem.* **1997**, *45*, 1991−1994.

(19) Jacobsen, C.; Schwarz, K.; Stockmann, H.; Meyer, A. S.; Adler-Nissen, J. Partitioning of Selected Antioxidants in Mayonnaise. *J. Agric. Food Chem.* **1999**, *47*, 3601−3610.

(20) Pekkarinen, S. S.; Stockmann, H.; Schwarz, K.; Heinonen, I. M.; Hopia, A. I. Antioxidant Activity and Partitioning of Phenolic Acids in Bulk and Emulsified Methyl Linoleate. *J. Agric. Food Chem.* **1999**, *47*, 3036−3043.

(21) Stockmann, H.; Schwarz, K.; Huynh-Ba, T. The Influence of Various Emulsifiers on the Partitioning and Antioxidant Activity of Hydroxylbenzoic Acids and Their Derivatives in Oil-in-Water Emulsions. *J. Am. Oil Chem. Soc.* **2000**, *77*, 535−542.

(22) Stockmann, H.; Schwarz, K. Partitioning of Low Molecular Weight Compounds in Oil-in-Water Emulsions. *Langmuir* **1999**, *15*, 6142−6149.

(23) Bunton, C. A.; Yao, J.; Romsted, L. S. Micellar Catalysis, A Useful Misnomer. *Curr. Opin. Colloid Interface Sci.* **1997**, *2*, 622−628.

(24) Bunton, C. A.; Romsted, L. S. Organic Reactivity in Microemulsions. In *Handbook of Microemulsion Science and Technology*; Kumar, P., Mittal, K. L., Eds.; Marcel Dekker: New York, 1999; pp 457−482.

(25) Romsted, L. S. Interfacial Composition of Surfactant Assemblies by Chemical Trapping with Arenediazonium Ions: Method and Applications. In *Reactions and Synthesis in Surfactant Systems*; J. Texter, Ed.; Marcel Dekker: New York, 2001; pp 265−294.

(26) Zollinger, H. *Diazo Chemistry I: Aromatic and Heteroaromatic Compounds*; VCH Publishers: Weinheim, 1994.

(27) Yao, J.; Romsted, L. S. Arenediazonium Salts: New Probes of the Compositions of Association Colloids. 7. Average Hydration Numbers and Cl− Concentrations in the Surfactant Film of Nonionic $C_{12}E_5$/Octane/Water Macroemulsions: Temperature and NaCl Concentration Effects. *Langmuir* **2000**, *16*, 8771−8779.

(28) Romsted, L. S.; Zhang, J. Determining Antioxidant Distributions in Model Food Systems: Development of a New Kinetic Method Based on the Pseudophase Model in Micelles and Opaque Emulsions. *Prog. Colloid Polym. Sci.* submitted for publication.

(29) Brown, K. C.; Doyle, M. P. Reduction of Arenediazonium Salts by Hydroquinone. Kinetics and Mechanism for the Electron-Transfer Step. *J. Org. Chem.* **1988**, *53*, 3255.

(30) Doyle, M. P.; Nesloney, C. L.; Shanklin, M. S.; Marsh, C. A.; Brown, K. C. Formation and Characterization of 3-*O*-Arenediazoascorbic Acids. New Stable Diazo Esters. *J. Org. Chem.* **1989**, *54*, 3785−3789.

(31) Reszka, K. J.; Chignell, C. F. EPR and Spin-Trapping Investigation of Free Radicals from the Reaction of 4-Methoxybenzenediazonium Tetrafluoroborate with Melanin and Melanin Precursors. *J. Am. Chem. Soc.* **1993**, *115*, 7752−7760.

(32) Reszka, K. J.; Chignell, C. F. One-electron Reduction of Arenediazonium Compounds by Physiological Electron Donors Generates Aryl Radicals. An EPR and Spin Trapping Investigation. *Chem.-Biol. Interact.* **1995**, *96*, 223−234.

(33) Chaudhuri, A.; Loughlin, J. A.; Romsted, L. S.; Yao, J. Arenediazonium Salts: New Probes of the Interfacial Compositions of Association Colloids. 1. Basic Approach, Methods and Illustrative Applications. *J. Am. Chem. Soc.* **1993**, *115*, 8351−8361.

(34) Romsted, L. S.; Yao, J. Arenediazonium Salts: New Probes of the Interfacial Compositions of Association Colloids. 4. Estimating Hydration Numbers of Aqueous Hexaethylene Glycol Mono Dodecyl Ether, $C_{12}E_6$, Micelles by Chemical Trapping. *Langmuir* **1996**, *12*, 2425−2432.

(35) Sepulveda, L.; Lissi, E.; Quina, F. Interactions of Neutral Molecules with Ionic Micelles. *Adv. Colloid Interface Sci.* **1986**, *25*, 1−57.

(36) Romsted, L. S. Rate Enhancements in Micellar Systems. Ph.D. Thesis, Indiana University, 1975.

(37) Romsted, L. S. A General Kinetic Theory of Rate Enhancements for Reactions between Organic Substrates and Hydrophilic Ions in Micellar Solutions. In *Micellization, Solubilization and Microemulsions*; Mittal, K. L., Ed.; Plenum Press: New York, 1977; pp 489−530.
(38) Berezin, I. V.; Martinek, K.; Yatsimirskii, A. K. Physicochemical Foundations of Micellar Catalysis. *Russ. Chem. Rev.* **1973**, *42*, 787−802.
(39) Minero, C.; Pramauro, E.; Pelizzetti, E. Electron-Transfer Reactions in Microemulsions. Oxidation of Benzenediols by Hexachloroiridate (IV). *Langmuir* **1988**, *4*, 101−105.
(40) da Rocha Pereira, R.; Zanette, D.; Nome, F. Application of the Pseudophase Ion-Exchange Model to Kinetics in Microemulsions of Anionic Detergents. *J. Phys. Chem.* **1990**, *94*, 356−361.
(41) Bunton, C. A.; Savelli, G. Organic Reactivity in Aqueous Micelles and Similar Assemblies. *Adv. Phys. Org. Chem.* **1986**, *22*, 213−309.
(42) Chaimovich, H.; Aleixo, F. M. V.; Cuccovia, I. M.; Zanette, D.; Quina, F. H. The Quantitative Analysis of Micellar Effects on Chemical Reactivity and Equilibria: An Evolutionary Overview. In *Solution Behavior of Surfactants: Theoretical and Applied Aspects*; Mittal, K. L., Fendler, E. J., Eds.; Plenum Press: New York, 1982; pp 949−973.
(43) Strey, R. Microemulsion Microstructure and Interfacial Curvature. *Colloid Polym. Sci.* **1994**, *272*, 1005−1019.
(44) Burauer, S.; Sachert, T.; Sottmann, T.; Strey, R. On Microemulsion Phase Behavior and The Monomeric Solubility of Surfactant. *Phys. Chem. Chem. Phys.* **1999**, *1*, 4299−4306.
(45) Eyer, P. Effects of Superoxide Dismutase on the Autoxidation of 1,4-Hydroquinone. *Chem.-Biol. Interact.* **1991**, *80*, 159−176.
(46) Reszka, K.; Bilski, P.; Chignell, C. F. EPR Spectra of DMPO Spin Adducts of Superoxide and Hydroxyl Radicals in Pyridine. *Free Radical Res. Commun.* **1992**, *17*, 377−385.
(47) Ruiz, M. A.; Garcia-Moreno, E.; Barbas, C.; Pingarron, J. M. Determination of Phenolic Antioxidants by HPLC with Amperometric Detection at a Nickel Phthalocyanine Polymer Modified Electrode. *Electroanalysis* **1999**, *11*, 470−474.
(48) Ruiz, M. A.; Reviejo, A. J.; Parrado, C.; Pingarron, J. M. Development of an Amperometric Enzyme Biosensor for the Determination of the Antioxidant *tert*-Butylanisole in a Medium of Reversed Micelles. *Electroanalysis* **1996**, *8*, 529−533.
(49) Gonzalez-Cortes, A.; Armisen, P.; Ruiz, M. A.; Yanezsedeno, P.; Pingarron, J. M. Electroanalytical Study of the Antioxidant *tert*-Butylhydroquinone (TBHQ) in an Oil-in-Water Emulsified Medium. *Electroanalysis* **1994**, *6*, 1014−1019.
(50) Bravo-Diaz, C.; Gonzalez-Romero, E. A novel method for the determination of vitamin C in natural orange juices by electrochemical monitoring of dediazoniation of 3-methylbenzenediazonium tetrafluoroborate. *Anal. Chim. Acta* **1999**, *385*, 373−384.
(51) Romero-Nieto, M. E.; Malvido-Hermelo, B.; Bravo-Diaz, C.; Gonzalez-Romero, E. Electrochemical Determination of Rate Constants and Product Yields for the Spontaneous Dediazoniation of *p*-Nitrobenzenediazonium Tetrafluoroborate in Acidic Aqueous Solution. *Int. J. Chem. Kinet.* **2000**, *32*, 419−430.
(52) Ugo, C.-C.; Gonzalez-Romero, E.; Bravo-Diaz, C. Effects of Ascorbic Acid on Arenediazonium Salts Reactivity: Kinetics and Mechanism of the Reaction. *Helv. Chim. Acta* **2001**, *84*, 632−648.
(53) Romsted, L. S. Micellar Effects on Reaction Rates and Equilibria. In *Surfactants in Solution*; Mittal, K. L., Lindman, B., Eds.; Plenum Press: New York, 1984; p 1015.
(54) Romsted, L. S. Quantitative Treatment of Benzimidazole Deprotonation Equilibria in Aqueous Micellar Solutions of Cetyltrimethylammonium Ion (CTAX, $X^- = Cl^-$, Br^-, and NO_3^-) Surfactants. 1. Variable Surfactant Concentration. *J. Phys. Chem.* **1985**, *89*, 5107−5113.
(55) Romsted, L. S. Quantitative Treatment of Benzimidazole Deprotonation Equilibria in Aqueous Micellar Solutions of Cetyltrimethylammonium Ion (CTAX, $X^- = Cl^-$, Br^-, and NO_3^-) Surfactants. 2. Effect of Added Salt. *J. Phys. Chem.* **1985**, *89*, 5113−5118.
(56) Romsted, L. S.; Zanette, D. Quantitative Treatment of Indicator Equilibria in Micellar Solutions of Sodium Decyl Phosphate and Sodium Lauryl Sulfate. *J. Phys. Chem.* **1988**, *92*, 4690−4698.

Received for review December 27, 2001. Revised manuscript received March 6, 2002. Accepted March 11, 2002. This is publication D10535-2-02 from the Center for Advanced Food Technology (CAFT). This research was supported in part by the State of New Jersey and the New Jersey Agricultural Experiment Station. The Center for Advanced Food Technology is a New Jersey Commission on Science and Technology Center. We are also grateful to the National Science Foundation, grant CHE-9985774, and NSF-International Programs, grant INT 97-22458, for partial support of this research.

JF011711Z